Nonlinear Dynamics and Systems Theory, **10** (2) (2010) 189–201

Optimal Guidance for Lunar Module Soft Landing

J.Y. Zhou [1*], K.L. Teo [1], D. Zhou [2] and G.H. Zhao [3]

[1] *Department of Mathematics and Statistics, Curtin University of Technology, Perth, 6102, Australia*
[2] *Department of Control Science and Engineering, Harbin Institute of Technology, Harbin, 150001, China*
[3] *Institute of Mathematical Sciences, Dalian University of Technology, DaLian, 116624, China*

Received: August 4, 2009; Revised: March 25, 2010

Abstract: In this paper, we consider an optimal control problem arising from the optimal guidance of a lunar module to achieving soft landing, where the description of the system dynamics is in a three-dimensional coordinate system. Our aim is to construct an optimal guidance law to realize the soft landing of the lunar module with the terminal attitude of the module to be within a small deviation from being vertical with respect to lunar surface, such that the fuel consumption and the terminal time are minimized. The optimal control problem is solved by applying the control parameterization technique and a time scaling transform. In this way, the optimal guidance law and the corresponding optimal descent trajectory are obtained. We then move on to consider an optimal trajectory tracking problem, where a desired trajectory is tracked such that the fuel consumption and the minimum time are minimized. This optimal tracking problem is solved using the same approach to the first optimal control problem. Numerical simulations demonstrate that the approach proposed is highly efficient.

Keywords: *optimal guidance law; lunar module; soft landing; optimal control with bounds on control and terminal states; control parameterization; time scaling transform; optimal trajectory tracking.*

Mathematics Subject Classification (2000): 49J15, 93C10, 93C15.

* Corresponding author: mailto:zhouhit@gmail.com

1 Introduction

Exploration of the moon, the nearest celestial body to the earth, is becoming more and more attractive for space scientists in recent years. Satellites and probes have been sent out to the moon for investigations. Generally speaking, there are three kinds of flight motions, i.e., flying over, circling or landing on the moon. Those missions aiming to land the lunar module safely on the surface of the moon are the most important ones.

The soft landing of the lunar module starts from the parking orbit of the moon, after Hohmann transfer the module enters into an elliptical orbit with the aposelene and perilune, which are, respectively, 110km and 15km away from the moon surface. When the module reaches the perilune, the powered descent soft landing begins. Normally, the lunar soft landing process from the perilune to the moon surface can mainly be divided into three phases. The first part is the powered deceleration phase, from 15km to 2km above the lunar surface, the module velocity is reduced to 0m/s by the propellant of the main thruster. The second part, from 2km to 100m above the lunar surface, is the attitude adjustment phase, and the module attitude is adjusted so that it is vertical to the moon surface. The last part is the vertical descent phase, a set of small thrusters is employed to cancel the moon gravity to ensure the module soft landing on the lunar surface vertically. In view of the fact that the surrounding circumstance of the moon is vacuum, lunar soft landing can not be performed in the same way as landing on the earth or mars. This is because the module can not depend on the lunar atmosphere for deceleration. One way of realizing soft landing is to use the reverse force thruster which will, however, consume much of the fuel that the lunar module is carrying. Clearly, if the fuel consumption can be reduced, then more payloads can be equipped. Thus, the optimal control strategy that guarantees the soft landing with least fuel consumption is highly in demand. Consequently, there are now many papers devoted to this area in the literature [1–6]. Meditch [7] discussed the problem of vertical lunar soft landing, where the thruster is operated at its maximum force. In this way, the mission is equivalent to a time optimal control problem and hence can be solved by existing theory. Wang [8] proposed a control scheme for achieving lunar soft landing, where the optimal control theory is used in combination with nonlinear neuro-control. Xi [9] presented an optimal control law obtained by utilizing Pontryagin Maximum Principle for the soft landing of a lunar module. Here, it is assumed that some of the control variables are not bounded. Liu [10] designed an optimal control strategy for the soft landing of a lunar module with a pre-specified terminal time by using the control parameterization technique and a time scaling transform. [1–3] and [7] studied the vertical descent phase of the lunar landing. In [4–6] and [8–10], the soft landing from the perilune to the moon surface is taken as a continuously powered descent process. However, none of these papers take into consideration the terminal angle constraint between the longitudinal axis of the module and the moon surface. In fact, among these research articles, the terminal angle of the module between its longitudinal axis and the plumb line is about fifty degree, which means that the module can not maintain a vertical attitude when it touches down on the ground. Furthermore, the dynamical system considered in most of these articles is in the two-dimensional polar coordinate system. The descent trajectory of the lunar module is assumed to remain in a vertical plane without consideration of the lateral movement. Neither the influence of the moon rotation is taken into account. However the lunar module, in practice, does not descend along such a vertical plane. To be realistic, the motion of the lunar module, which takes into consideration moon rotation, should be

described in a three-dimensional coordinate system [11].

The problem of the soft landing of a lunar module at the minimum time with the least fuel consumption can be formulated as an optimal control problem with constraints on the control and the terminal states. However, it is much too complex to be solved by using Pontryagin Maximum Principle. In this paper, we calculate the optimal descent trajectory of the lunar module by using the control parameterization technique in conjunction with a time scaling transform [12]. The lunar soft landing is treated as a continuously powered descent process with a constraint on the angle of the module between its longitudinal axis and the moon surface. During the entire process of the lunar landing, only the main reverse force thruster is needed for deceleration. Therefore, the design complexity of the guidance control law is reduced substantially. By applying the control parameterization technique and the time scaling transform, the optimal control problem is approximated by a sequence of optimal parameter selection problems. Each of which is basically a mathematical programming problem and hence can be solved by existing gradient-based optimization methods [13–15]. A general purpose optimal control software package, called MISER 3.3 [15], was developed based on these methods. We make use of this optimal control software package to solve our problem in this paper. The optimal trajectory tracking problem, where a desired trajectory is to be tracked with the least fuel consumption in the minimum time, is also considered and the same approach to the first optimal control problem is utilized to solve such an optimal trajectory tracking problem.

2 Problem Formulation

For continuously powered descent soft landing, the reverse force thruster begins to work, starting from the perilune to decelerate the initial velocity of the module. With the cooperation of the attitude control thrusters, the module is guided to reach the landing target vertically with a small and safe final velocity. In this paper, we study the optimal guidance scheme for ensuring the soft landing of the lunar module from the perilune to the moon surface.

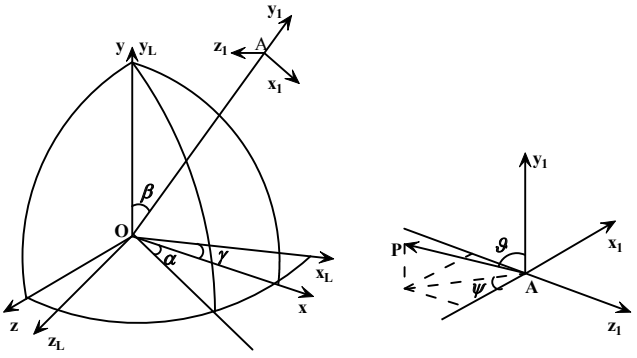

Figure 2.1: Coordinate systems.

As the influences of other celestial bodies on the lunar module are small, compared with the moon gravity, the lunar module soft landing can be treated in a two-body system [16]. The motion of the lunar module soft landing is described in a three-dimensional coordinate system (Figure 2.1). Suppose $oxyz$ and $ox_Ly_Lz_L$ are, respectively, the Lunar

Central Inertial Coordinate and Lunar Fixed Coordinate with the moon equator as the reference plane. $Ax_1y_1z_1$ is the orbit coordinate, A is the position of the lunar module. The three coordinates form a right handed system. α and β represent, respectively, the rotation angles between $oxyz$ and $Ax_1y_1z_1$. The direction of the thrust force P in the coordinate $Ax_1y_1z_1$ can be described in terms of ϑ and ψ. γ is the rotation angle between $oxyz$ and $ox_Ly_Lz_L$. Without lose of generality, we assume that $oxyz$ and $ox_Ly_Lz_L$ coincide with each other at the beginning of the soft landing. Based on Newton's second law, system dynamic equations can be derived to give [11]

$$\begin{cases} \dot{x}_L = V_{xL}, \\ \dot{y}_L = V_{yL}, \\ \dot{z}_L = V_{zL}, \\ \dot{V}_{xL} = BQV_r/m + g_{xL} - 2\omega_L V_{zL}, \\ \dot{V}_{yL} = CQV_r/m + g_{yL}, \\ \dot{V}_{zL} = DQV_r/m + g_{zL} + 2\omega_L V_{xL}, \\ \dot{m} = -Q, \end{cases} \tag{2.1}$$

where

$$\begin{aligned} B &= (\cos\alpha\cos\beta\cos\gamma - \sin\alpha\sin\gamma)\sin\vartheta\cos\psi \\ &\quad -(\sin\alpha\cos\beta\cos\gamma + \cos\alpha\sin\gamma)\sin\vartheta\sin\psi + \sin\beta\cos\gamma\cos\vartheta, \\ C &= -\cos\alpha\sin\beta\sin\vartheta\cos\psi + \cos\beta\cos\vartheta + \sin\alpha\sin\beta\sin\vartheta\sin\psi, \\ D &= (\cos\alpha\cos\beta\sin\gamma + \sin\alpha\cos\gamma)\sin\vartheta\cos\psi \\ &\quad -(\sin\alpha\cos\beta\sin\gamma - \cos\alpha\cos\gamma)\sin\vartheta\sin\psi + \sin\beta\sin\gamma\cos\vartheta. \end{aligned}$$

while x_L, y_L, z_L and V_{xL}, V_{yL}, V_{zL} are the positions and velocities in the Lunar Fixed Coordinate. m is the mass of the lunar module, Q and V_r represent, respectively, the fuel consumption rate and the specific impulse of the thruster, g_{xL}, g_{yL}, and g_{zL} denote the components of lunar gravity in $ox_Ly_Lz_L$, and ω_L is the angular velocity of the moon rotation.

Introduce two new state equations

$$\dot{\vartheta} = v, \tag{2.2}$$

$$\dot{\psi} = w \tag{2.3}$$

and let

$$\begin{aligned} \boldsymbol{x} &= [x_L, y_L, z_L, V_{xL}, V_{yL}, V_{zL}, \vartheta, \psi, m]^T \\ &= [x_1, x_2, x_3, x_4, x_5, x_6, x_7, x_8, x_9]^T, \end{aligned}$$

$$\boldsymbol{u} = [Q, v, w]^T = [u_1, u_2, u_3]^T.$$

The original system dynamics (2.1) can be rewritten in the form of an affine nonlinear system given below.

$$\dot{\boldsymbol{x}}(t) = \boldsymbol{f}(\boldsymbol{x}(t)) + \boldsymbol{B}(\boldsymbol{x}(t))\boldsymbol{u}(t), \tag{2.4}$$

where

$$\boldsymbol{f}(\boldsymbol{x}) = [x_4, x_5, x_6, g_{xL} - 2\omega_L x_6, g_{yL}, g_{zL} + 2\omega_L x_4, 0, 0, 0]^T, \tag{2.5}$$

$$\boldsymbol{B}(\boldsymbol{x}) = \begin{bmatrix} 0 & 0 & 0 & M_1 & M_2 & M_3 & 0 & 0 & -1 \\ 0 & 0 & 0 & 0 & 0 & 0 & 1 & 0 & 0 \\ 0 & 0 & 0 & 0 & 0 & 0 & 0 & 1 & 0 \end{bmatrix}^T \tag{2.6}$$

while

$$\begin{aligned} M_1 &= [(\cos\alpha\cos\beta\cos\gamma - \sin\alpha\sin\gamma)\sin x_7\cos x_8 \\ &\quad -(\sin\alpha\cos\beta\cos\gamma + \cos\alpha\sin\gamma)\sin x_7\sin x_8 + \sin\beta\cos\gamma\cos x_7]V_r/x_9, \\ M_2 &= [-\cos\alpha\sin\beta\sin x_7\cos x_8 + \cos\beta\cos x_7 + \sin\alpha\sin\beta\sin x_7\sin x_8]V_r/x_9, \end{aligned}$$

and

$$\begin{aligned} M_3 &= [(\cos\alpha\cos\beta\sin\gamma + \sin\alpha\cos\gamma)\sin x_7\cos x_8 \\ &\quad -(\sin\alpha\cos\beta\sin\gamma - \cos\alpha\cos\gamma)\sin x_7\sin x_8 + \sin\beta\sin\gamma\cos x_7]V_r/x_9. \end{aligned}$$

The boundedness constraints on the control vector $\boldsymbol{u} = [u_1, u_2, u_3]^T$ are specified below:

$$\boldsymbol{\alpha} \le \boldsymbol{u}(t) \le \boldsymbol{\beta},\ \forall\ t \ge 0, \tag{2.7}$$

where $\boldsymbol{\alpha} = [\alpha_1, \alpha_2, \alpha_3]^T$ and $\boldsymbol{\beta} = [\beta_1, \beta_2, \beta_3]^T$, while $\alpha_i,\ i = 1, 2, 3$, and $\beta_i,\ i = 1, 2, 3$, are given constants. Let $\mathcal{U}$ be the set of all such controls. Elements from $\mathcal{U}$ are called admissible controls and $\mathcal{U}$ is referred to as the class of admissible controls.

The initial conditions of the soft landing are determined by the state of the lunar module in the perilune at the initial time $t_0 = 0$. The terminal constraints are specified by the requirement of the soft landing, i.e., when the lunar module reaches the target at the terminal time t_f which is free, its velocity should be close to zero and its longitudinal axis should be close to vertical to the moon surface. So the initial conditions and terminal state constraints can be expressed as:

$$\boldsymbol{x}(t_0) = [x_{L0}, y_{L0}, z_{L0}, V_{xL0}, V_{yL0}, V_{zL0}, \vartheta_0, \psi_0, m_0]^T \tag{2.8}$$

and

$$\boldsymbol{\Phi} = \begin{bmatrix} x_L(t_f) - x_{Lr} \\ y_L(t_f) - y_{Lr} \\ z_L(t_f) - z_{Lr} \\ V_{xL}(t_f) - 0 \\ V_{yL}(t_f) - 0 \\ V_{zL}(t_f) - 0 \end{bmatrix} = 0, \tag{2.9}$$

$$\vartheta_{t_f} \le x_7(t_f) \le 0, \tag{2.10}$$

where $(x_{Lr},\ y_{Lr},\ z_{Lr})$ represents the position of the landing target in the Lunar Fixed Coordinate, ϑ_{t_f} is the terminal separation angle of the module between its longitudinal axis and the direction of the plumb line. Our aim is to design an optimal control strategy to achieve the task of soft landing of the lunar module such that conditions (2.9) and (2.10) are satisfied and the fuel consumption and the flying time are minimized. The task of minimizing the fuel consumption and the flying time is formulated as the task of minimizing the following cost function

$$J = m_0 - x_9(t_f) + t_f. \tag{2.11}$$

We may now formally state our optimal control problem as follows.
Problem (P): Given system (2.4), find a control $\boldsymbol{u} \in \mathcal{U}$ such that the cost function (2.11) is minimized subject to the control constraint (2.7), the initial condition (2.8) and the terminal state constraints (2.9) and (2.10).

3 Parameterization of the Control

To solve Problem (P), we shall utilize the control parameterization technique to approximate the control vector $\boldsymbol{u}$ with piecewise constant functions over the time interval $[0, t_f]$ as:

$$u_1^p(t) = \sum_{k=1}^{n_p} \sigma_1^k \chi_{[\tau_{k-1}, \tau_k)}(t), \tag{3.1}$$

$$u_2^p(t) = \sum_{k=1}^{n_p} \sigma_2^k \chi_{[\tau_{k-1}, \tau_k)}(t), \tag{3.2}$$

$$u_3^p(t) = \sum_{k=1}^{n_p} \sigma_3^k \chi_{[\tau_{k-1}, \tau_k)}(t), \tag{3.3}$$

where

$$\tau_0, \tau_1, \ldots, \tau_{n_p},\ \tau_{k-1} < \tau_k,\ k = 1, 2, \ldots, n_p \tag{3.4}$$

(with $\tau_0 = 0$ and $\tau_{n_p} = t_f$) are partition points of the time interval $[0, t_f]$, and $\chi_I(t)$ denotes the indicator function of I defined by

$$\chi_I(t) = \begin{cases} 1,\ t \in I, \\ 0,\ \text{elsewhere.} \end{cases} \tag{3.5}$$

Let $\boldsymbol{\tau} = [\tau_1, \ldots, \tau_{n_p}]^T$ and let Υ^p be the set which consists of all such $\boldsymbol{\tau}$. For each $j = 1, 2, 3$, and $k = 1, 2, \ldots, n_p$, σ_j^k is a constant control parameter, and τ_k , $k = 1, \ldots, n_p - 1$, are the switching times. Let $\boldsymbol{\sigma}_j = [\sigma_j^1, \cdots, \sigma_j^{n_p}]^T$, $j = 1, 2, 3$, and let $\boldsymbol{\sigma} = [(\boldsymbol{\sigma}_1)^T, (\boldsymbol{\sigma}_2)^T, (\boldsymbol{\sigma}_3)^T]^T$. Define $\boldsymbol{u}^p = [u_1^p, u_2^p, u_3^p]^T$.

As $\boldsymbol{u}^p \in \boldsymbol{\mathcal{U}}$, it is clear that

$$\alpha_j \le \sigma_j^k \le \beta_j \tag{3.6}$$

for $j = 1, 2, 3$, and $k = 1, 2, \ldots, n_p$. Let Ξ^p denote the set containing all such $\boldsymbol{\sigma}$. Here, for the soft landing of a lunar module, the terminal time $\tau_{n_p} = t_f$ is unknown and regarded as a decision variable.

We shall map all these variable time points τ_k, $k = 1, \ldots, n_p$, into fixed time points ς_k, $k = 1, \ldots, n_p$, in a new time horizon $[0,\ 1]$, such that

$$0 = \varsigma_0 < \varsigma_1 < \cdots < \varsigma_{n_p - 1} < \varsigma_{n_p} = 1. \tag{3.7}$$

For this, we introduce a new state equation defined on $[0,\ 1]$

$$\frac{dt(s)}{ds} = \mu^p(s), \tag{3.8}$$

where $t(0) = 0$, $t(1) = t_f$,

$$\mu^p(s) = \sum_{k=1}^{n_p} \delta_k \chi_{[\varsigma_{k-1}, \varsigma_k)}(s). \tag{3.9}$$

Here,

$$\delta_k \ge 0,\ k = 1, \ldots, n_p, \tag{3.10}$$

are decision variables. $\mu^p(s)$ is called the time scaling control. It is a nonnegative piecewise constant function with possible discontinuities at the pre-fixed knots ς_k, $k = 1, \ldots, n_p - 1$. Let $\boldsymbol{\delta} = [\delta_1, \cdots, \delta_{n_p}]^T$.

By applying the time scaling transform (3.8), system equations (2.4) and (3.8) are transformed into

$$\frac{d\tilde{\boldsymbol{x}}(s)}{ds} = \begin{bmatrix} \mu^p(s)[\boldsymbol{f}(t(s),\hat{\boldsymbol{x}}(s)) + \boldsymbol{B}(t(s),\hat{\boldsymbol{x}}(s))\hat{\boldsymbol{u}}^p(s)] \\ \mu^p(s) \end{bmatrix}, \tag{3.11}$$

where $\tilde{\boldsymbol{x}} = [\tilde{x}_1, \cdots, \tilde{x}_9, \tilde{x}_{10}]^T = [(\hat{\boldsymbol{x}})^T, t]^T$, $\hat{\boldsymbol{x}}(s) = \boldsymbol{x}(t(s))$, and $\hat{\boldsymbol{u}}^p(s) = \boldsymbol{u}(t(s))$ given by

$$\hat{\boldsymbol{u}}^p(s) = \sum_{k=1}^{n_p} \boldsymbol{\sigma}^k \chi_{[\varsigma_{k-1},\varsigma_k)}(s). \tag{3.12}$$

The initial condition is

$$\tilde{\boldsymbol{x}}(0) = [x_{L0}, y_{L0}, z_{L0}, V_{xL_0}, V_{yL_0}, V_{zL0}, \vartheta_0, \psi_0, m_0, 0]^T. \tag{3.13}$$

The cost function (2.11) and the terminal constraints (2.9) and (2.10) become

$$\tilde{J} = m_0 - \tilde{x}_9(1) + \tilde{x}_{10}(1) \tag{3.14}$$

and

$$\tilde{\boldsymbol{\Phi}} = \begin{bmatrix} \tilde{x}_1(1) - x_{Lr} \\ \tilde{x}_2(1) - y_{Lr} \\ \tilde{x}_3(1) - z_{Lr} \\ \tilde{x}_4(1) - 0 \\ \tilde{x}_5(1) - 0 \\ \tilde{x}_6(1) - 0 \\ \tilde{x}_{10}(1) - t_f \end{bmatrix} = 0, \tag{3.15}$$

$$\vartheta_{t_f} \le \tilde{x}_7(1) \le 0, \tag{3.16}$$

respectively. They can be written in canonical form as:

$$\tilde{g}_0(\boldsymbol{\sigma},\boldsymbol{\delta}) = \tilde{\Phi}_0(\tilde{x}(1|\boldsymbol{\sigma},\boldsymbol{\delta}),\ \boldsymbol{\sigma},\boldsymbol{\delta}) + \int_0^1 \tilde{\ell}_0(s,\ \tilde{x}(s|\boldsymbol{\sigma},\boldsymbol{\delta}),\ \boldsymbol{\sigma},\boldsymbol{\delta})ds \tag{3.17}$$

and

$$\tilde{g}_i(\boldsymbol{\sigma},\boldsymbol{\delta}) = \tilde{\Phi}_i(\tilde{x}(1|\boldsymbol{\sigma},\boldsymbol{\delta}),\ \boldsymbol{\sigma},\boldsymbol{\delta}) + \int_0^1 \tilde{\ell}_i(s,\ \tilde{x}(s|\boldsymbol{\sigma},\boldsymbol{\delta}),\ \boldsymbol{\sigma},\boldsymbol{\delta})ds = 0, \quad i = 1, ..., 7, \tag{3.18}$$

$$\tilde{g}_i(\boldsymbol{\sigma},\boldsymbol{\delta}) = \tilde{\Phi}_i(\tilde{x}(1|\boldsymbol{\sigma},\boldsymbol{\delta}),\ \boldsymbol{\sigma},\boldsymbol{\delta}) + \int_0^1 \tilde{\ell}_i(s,\ \tilde{x}(s|\boldsymbol{\sigma},\boldsymbol{\delta}),\ \boldsymbol{\sigma},\boldsymbol{\delta})ds \le 0, \quad i = 8, 9, \tag{3.19}$$

where $\tilde{\ell}_i = 0$, for $i = 0, 1, ..., 9,$, while $\tilde{\Phi}_i$, $i = 0, 1, ..., 9$, are defined by (3.14), (3.15) and (3.16), respectively.

The original optimal control problem is now approximated by a sequence of optimal parameter selection problems depending on p, the number of the partition points of the time horizon $[0,\ t_f]$, given below.

Problem ($\tilde{\mathrm{P}}(p)$): Given system (3.11) with the initial condition (3.13) on the time interval $s \in [0\ ,\ 1]$, find a control parameter vector $\boldsymbol{\sigma} \in \Xi^p$ and a switching time vector $\boldsymbol{\delta} \in \Upsilon^p$, such that the cost function (3.14) is minimized subject to the terminal constraints (3.15) and (3.16).

For each p, Problem $(\tilde{\mathrm{P}}(p))$ can be solved as a nonlinear optimization problem where the cost function (3.14) is minimized subject to the terminal constraints (3.15) and (3.16) and the constraints on the decision vectors $\boldsymbol{\sigma}$ and $\boldsymbol{\delta}$ given by (3.6) and (3.10), where the dynamical system (3.11) is used to generate the values of the cost function (3.14) and the constraint functions (3.15) and (3.16). Existing gradient-based optimization methods can be used to solve Problem $(\tilde{\mathrm{P}}(p))$. For this, we need the gradient formulas of the objective function and the constraint functions. For the constraints (3.6) and (3.10), their gradient formulas are straightforward to calculate. The gradient formulas of the objective function (3.14) and the constraint functions (3.15) and (3.16) are given bellow.

Theorem 3.1 [12] *For each $i = 0, 1, \ldots, 9$, the gradient of the function $\tilde{g}_i$ with respect to $\boldsymbol{\sigma}$ and $\boldsymbol{\delta}$ are given by*

$$\frac{\partial \tilde{g}_i(\boldsymbol{\sigma}, \boldsymbol{\delta})}{\partial \boldsymbol{\sigma}} = \int_0^1 \frac{\partial \tilde{H}_i(s, \tilde{\boldsymbol{x}}(s), \boldsymbol{\sigma}, \boldsymbol{\delta}, \tilde{\boldsymbol{\lambda}}^i(s|\boldsymbol{\sigma}, \boldsymbol{\delta}))}{\partial \boldsymbol{\sigma}} ds \tag{3.20}$$

and

$$\frac{\partial \tilde{g}_i(\boldsymbol{\sigma}, \boldsymbol{\delta})}{\partial \boldsymbol{\delta}} = \int_0^1 \frac{\partial \tilde{H}_i(s, \tilde{\boldsymbol{x}}(s), \boldsymbol{\sigma}, \boldsymbol{\delta}, \tilde{\boldsymbol{\lambda}}^i(s|\boldsymbol{\sigma}, \boldsymbol{\delta}))}{\partial \boldsymbol{\delta}} ds, \tag{3.21}$$

where

$$\tilde{H}_i(s, \tilde{\boldsymbol{x}}, \boldsymbol{\sigma}, \boldsymbol{\delta}, \tilde{\boldsymbol{\lambda}}^i) = \tilde{\ell}_i(s, \tilde{\boldsymbol{x}}, \boldsymbol{\sigma}, \boldsymbol{\delta}) + (\tilde{\boldsymbol{\lambda}}^i)^T \tilde{\boldsymbol{f}}(s, \tilde{\boldsymbol{x}}, \boldsymbol{\sigma}, \boldsymbol{\delta}) \tag{3.22}$$

and, for each $i = 0, 1, \ldots, 9$, $\tilde{\boldsymbol{\lambda}}^i(s|\boldsymbol{\sigma}, \boldsymbol{\delta})$ is the solution of the following co-state system corresponding to $(\boldsymbol{\sigma}, \boldsymbol{\delta})$:

$$\frac{d(\tilde{\boldsymbol{\lambda}}(s))^T}{ds} = -\frac{\partial \tilde{H}_i(s, \tilde{\boldsymbol{x}}(s|\boldsymbol{\sigma}, \boldsymbol{\delta}), \boldsymbol{\sigma}, \boldsymbol{\delta}, \tilde{\boldsymbol{\lambda}}(s))}{\partial \tilde{\boldsymbol{x}}}, \ s \in [0, 1) \tag{3.23}$$

with

$$(\tilde{\boldsymbol{\lambda}}(1))^T = \frac{\partial \tilde{\Phi}_i(\tilde{\boldsymbol{x}}(1|\boldsymbol{\sigma}, \boldsymbol{\delta}))}{\partial \tilde{\boldsymbol{x}}}. \tag{3.24}$$

Proof The proof of Theorem 3.1 is similar to that given for Theorem 5.2.1 of [12].

For each p, Problem $(\tilde{\mathrm{P}}(p))$ is an optimal parameter selection problem, which can be viewed as a nonlinear optimization problem. The gradient formulas of the cost function (3.17) and the constraint functions (3.18) and (3.19) are given in Theorem 3.1, while the constraints (3.6) are just the bounds for these control parameter vectors.

Thus, any existing gradient-based optimization method, such as sequential quadratic programming algorithm [17], can be used to solve Problem $(\tilde{\mathrm{P}}(p))$. The optimal control software MISER 3.3 was implemented based on these ideas. It is used in this paper to solve our optimal control problem. Intuitively, the larger the p, the closer Problem $(\tilde{\mathrm{P}}(p))$ is to Problem (P). This intuition is true. We shall briefly discuss the convergence issue as follows. Let $(\boldsymbol{\sigma}^{p,*}, \boldsymbol{\delta}^{p,*})$ be the optimal parameter vector of Problem $(\tilde{\mathrm{P}}(p))$, and let $\tilde{\boldsymbol{u}}^{p,*}$ be the corresponding piecewise constant control given by

$$\tilde{\boldsymbol{u}}^{p,*}(s) = \sum_{k=1}^{n_p} \boldsymbol{\sigma}^{p,*} \chi_{[\frac{k-1}{n_p}, \frac{k}{n_p})}(s), \tag{3.25}$$

where

$$\tilde{\boldsymbol{u}}^{p,*} = [\tilde{u}_1^{p,*}, \tilde{u}_2^{p,*}, \tilde{u}_3^{p,*}]^T, \tag{3.26}$$

$$\boldsymbol{\sigma}^{p,*} = [(\boldsymbol{\sigma}_1^{p,*})^T, (\boldsymbol{\sigma}_2^{p,*})^T, (\boldsymbol{\sigma}_3^{p,*})^T]^T, \tag{3.27}$$

$$\boldsymbol{\delta}^{p,*} = [\delta_1^{p,*}, \ldots, \delta_{n_p}^{p,*}]^T. \tag{3.28}$$

In the original time horizon $[0, t_f]$, we have

$$\boldsymbol{u}^{p,*}(t) = \sum_{k=1}^{n_p} \boldsymbol{\sigma}^{p,*} \chi_{[\tau_{k-1}^{p,*}, \tau_k^{p,*})}(t), \tag{3.29}$$

where

$$\tau_i^{p,*} = \sum_{k=1}^{i} \delta_k^{p,*}, \quad i = 1, \ldots, n_p. \tag{3.30}$$

Furthermore, let $\boldsymbol{u}^*$ be the optimal control of Problem (P). Then, by virtue of the discussion presented in Section 5 on Convergence Analysis of [18], it holds that
(i) $g_0(\boldsymbol{u}^{p,*}) \to g_0(\boldsymbol{u}^*)$;
(ii) if $\boldsymbol{u}^{p,*} \to \tilde{\boldsymbol{u}}$ almost everywhere in $[0, t_f]$, then $\tilde{\boldsymbol{u}}$ is an optimal control of Problem (P).

From our extensive simulation study experience, we observe that p does not need to be chosen to be too large. In fact, the difference in the cost values between $p = 20$ and those with larger p is, in general, very insignificant. Thus, $p = 20$ is chosen in our numerical simulation.

4 Optimal Trajectory Tracking

We now move on to consider a situation for which the spacecraft is required to track a desired trajectory, such that the fuel consumption and the terminal time are minimized. To realize such an optimal tracking control problem, we only need to modify the cost function J of Problem (P) as:

$$J = m_0 - x_9(t_f) + t_f + \int_0^{t_f} [(x_1(t) - \bar{x}_r(t))^2 + (x_2(t) - \bar{y}_r(t))^2 + (x_3(t) - \bar{z}_r(t))^2]dt, \tag{4.1}$$

where $(\bar{x}_r,\ \bar{y}_r,\ \bar{z}_r)$ denotes the desired reference trajectory. Let this optimal trajectory control problem be referred to as Problem (Q). Using the control parameterization technique and the time scaling transform as described in Section 3, Problem (Q) is transformed into Problem $(\tilde{\mathrm{Q}}(p))$, where the transformed cost function

$$\tilde{J} = m_0 - \tilde{x}_9(1) + \tilde{x}_{10}(1) + \int_0^1 [(\tilde{x}_1(s) - \hat{x}_r(s))^2 + (\tilde{x}_2(s) - \hat{y}_r(s))^2 + (\tilde{x}_3(s) - \hat{z}_r(s))^2]ds \tag{4.2}$$

is to be minimized over $(\Xi^p \times \Upsilon^p)$ subject to the system dynamic (3.11) with initial condition (3.13) and the terminal state constraints (3.15) and (3.16), where $\hat{x}_r(s) = \bar{x}_r(t(s))$, $\hat{y}_r(s) = \bar{y}_r(t(s))$, $\hat{z}_r(s) = \bar{z}_r(t(s))$.

The gradient formulas of the cost function (4.2) and constraint functions (3.15) and (3.16) can be derived in the same way as those of Problem $(\tilde{\mathrm{P}}(p))$ given in Theorem 3.1. The optimal control parameter selection problem $(\tilde{\mathrm{Q}}(p))$ is thus solved utilizing the optimal control software MISER 3.3.

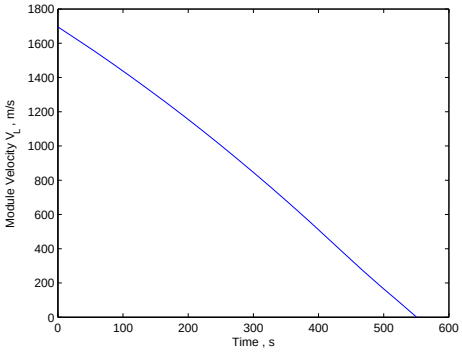

Figure 5.1: Module velocity V_L.

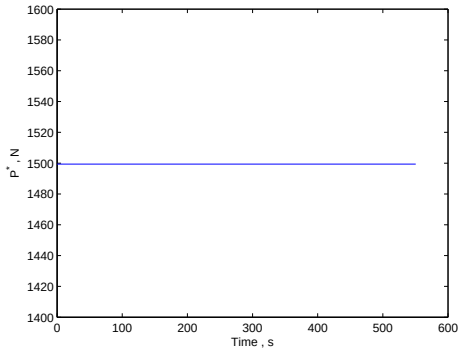

Figure 5.2: Thrust force P^*.

5 Numerical Simulations

The initial conditions of the lunar module are given as: $x_{L0} = 8.19371 \times 10^5$m, $y_{L0} = 1.428867 \times 10^6$m, $z_{L0} = 5.996306 \times 10^5$m, $V_{xL0} = 1115$m/s, $V_{yL0} = -981.82$m/s, $V_{zL0} = 816$m/s, $m_0 = 600$kg. At the initial time of the soft landing, the rotation angle $\gamma(t_0) = 0°$. Specific impulse $V_r = 300 \times 9.8$m/s and angular velocity of the moon rotation $\omega_L = 2.661699 \times 10^{-6}$rad/s.

We first consider the task of achieving the soft landing of the lunar module. The landing target is in Mare Imbrium on the moon surface, which is located at 38.628° North latitude and 36.806° West longitude. Control variables are chosen subject to the bounds: $0 \text{ kg/s} \le \sigma_1^k \le 0.51 \text{ kg/s}$, $\left|\sigma_2^k\right| \le 1 \ °/\text{s}$, $\left|\sigma_3^k\right| \le 1 \ °/\text{s}$, $k = 1, 2, \ldots, n_p$. Terminal separation angle of the module between its longitudinal axis and the plumb line is $\vartheta_{t_f} = 5°$. The scaled time interval is $s \in [0, 1]$ partitioned into 20 equal subintervals. Terminal time of the soft landing is free to vary. The corresponding optimal parameter selection problem is then solved by using the software MISER 3.3. Terminal conditions of the lunar module obtained are listed below.

$$x_L(t_f) = 1.0871218 \times 10^6 m, \ y_L(t_f) = 1.0849749 \times 10^6 m, \ z_L(t_f) = 8.134568 \times 10^5,$$

$$V_{xL}(t_f) = 1 \times 10^{-4}\text{m/s}, \ V_{yL}(t_f) = 0\text{m/s}, \ V_{zL}(t_f) = 2 \times 10^{-4}\text{m/s}.$$

Figure 5.1 shows the time history in the original time horizon $[0, \ t_f]$ of the lunar module velocity. We see that it converges smoothly to zero as the module lands on the moon. Figures 5.2, 5.4 and 5.6 are optimal control outputs during the period of soft landing, also in the original time horizon $[0, \ t_f]$. Here, we see that the reverse force thruster works at its maximum thrust force all the time, while the two angular velocity controllers are operating within their bounds. Under the optimal control law, the lunar module is guided to the target precisely, and the optimal descent trajectory is shown in Figure 5.3. Terminal mass of the module is 319.2728kg. Figure 5.5 depicts the time scaling control. Lunar module lands on the moon surface vertically after 550.4455s, with the terminal separation angle between the module longitudinal axis and the plumb line $\vartheta(t_f) = -4.998°$.

Our next task is to investigate the mission of the optimal trajectory tracking. Suppose the desired trajectory is the one obtained from the solution of Problem (P). Suppose that the initial position of the lunar module is given as $x_{L0} = 8.18348 \times 10^5$m, $y_{L0} = 1.428821 \times 10^6$m, $z_{L0} = 6.01136 \times 10^5$m, which are different from those for Problem (P).

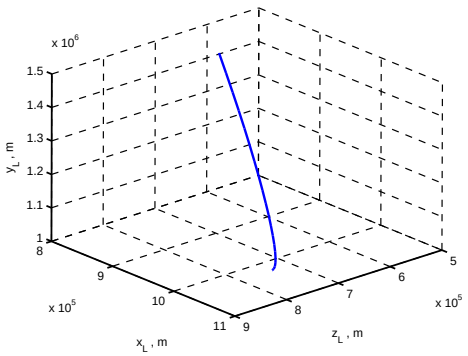

Figure 5.3: Optimal descent trajectory.

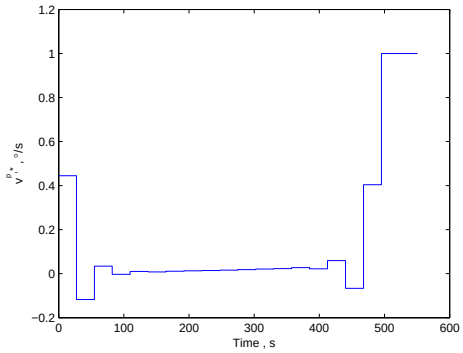

Figure 5.4: Angular velocity $v^{p,*}$.

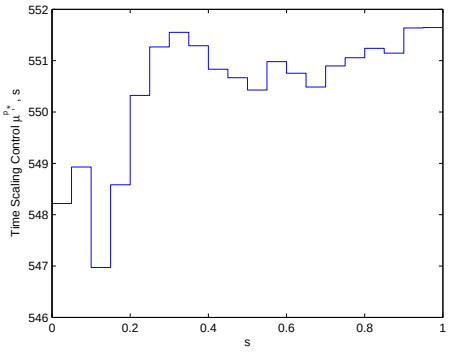

Figure 5.5: Time scaling control $\mu^{p,*}$.

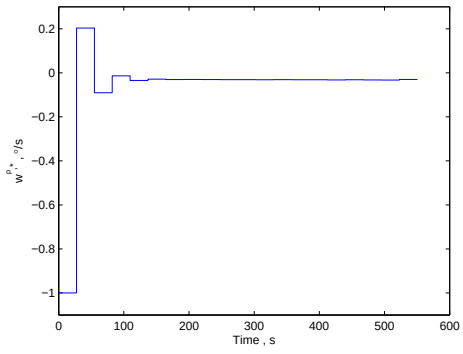

Figure 5.6: Angular velocity $w^{p,*}$.

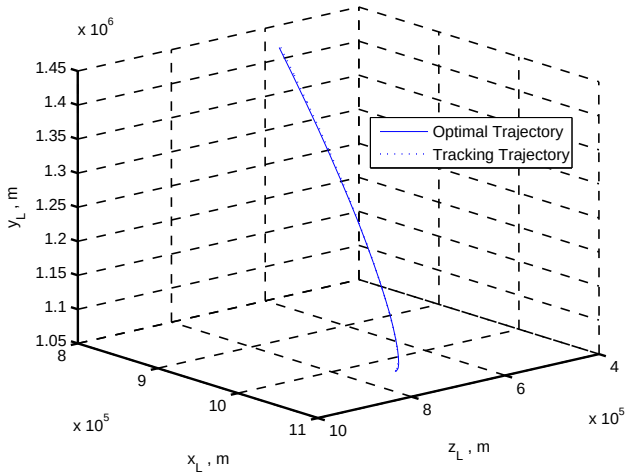

Figure 5.7: Optimal trajectory tracking.

Let this optimal tracking problem be referred to as Problem (Q). It is solved by using the approach detailed in Section 4, where the optimal control software MISER 3.3 is utilized. The optimal control obtained for Problem (P) is used as the initial guess for the search of the optimal control of Problem (Q). Let the optimal control of Problem (Q) obtained be denoted as $\boldsymbol{\upsilon}^*$. Then, under this control, the Lunar module is guided to the target at the terminal time $t_f = 572.8$s. The terminal velocity is 6.2e-4m/s, while the terminal mass is 315.43kg. From Figure 5.7, we see that the optimal trajectory tracks the desired trajectory satisfactorily.

6 Conclusions

This paper studied the soft landing of the lunar module, where its system dynamics is described in a three-dimensional coordinate system. The constraints on the control and the terminal state are also taken into consideration. By using the control parameterization technique and the time scaling transform, the optimal control problem is solved as an optimal parameter selection problem by the optimal control software package MISER 3.3, yielding an optimal control law. This optimal control law steers the lunar module to achieve the pre-specified landing target precisely such that the fuel consumption and the terminal time are minimized. The module touches down on the moon vertically with reference to lunar surface. The task of optimal trajectory tracking was also formulated and solved. The proposed approach is highly effective.

References

[1] Ma, K.M., Chen, L.J. and Wang, Z.C. Practical design of control law for flight vehicle soft landing. *Missiles and Space Vehicles* (2) (2001) 39–43.

[2] Ruan, X.G. A nonlinear nuerocontrol scheme for lunar soft landing. *Journal of Astronautics* **19**(1) (1998) 35–43.

[3] Hebertt, S.R. Soft landing on a planet: a trajectory planning approach for the liouvillian model. *Proceedings of American Control Conference* (1999) 2936–2940.

[4] Wang, D.Y., Li, T.S. and Ma, X.R. Numerical solution of TPBVP in optimal lunar soft landing. *Aerospace Control* (3) (2000) 44–49.

[5] Xu, M. and Li, J.F. Optimal control of lunar soft landing. *Journal of Tsinghua University (Science and Technology)* **41**(8) (2001) 87–89.

[6] Wang, Z., Li, J.F., Cui, N.G. and Liu, T. Genetic algorithm optimization of lunar probe soft landing trajectories. *Journal of Tsinghua University (Science and Technology)* **43**(8) (2003) 1056–1059.

[7] Meditch, S.J. On the problem of optimal thrust programming for a lunar soft landing. *IEEE Transaction on Automatic Control* **9**(4) (1964) 477–484.

[8] Wang, D.Y., Li, T.S., Yan, H. and Ma, X.R. Neuro-optimal guidance control for lunar module soft landing. *Journal of Systems Engineering and Electronics* **10**(3) (1999) 22–31.

[9] Xi, X.N., Zeng, G.Q. Ren, X. and Zhao, H.Y. *Orbit design of lunar probe*. National Defence Industry Press, Beijing, 2001.

[10] Liu, X.L., Duan, G.R. and Teo, K.L. Optimal soft landing control for moon lander. *Automatica* **44**(4) (2008) 1097–1103.

[11] Zhou, J.Y. and Zhou, D. Precise modeling and optimal orbit design of lunar modules soft landing. *Journal of Astronautics* **28**(6) (2007) 1462–1466.

[12] Teo, K.L., Goh, C.J. and Wong, K.H. *A unified computational approach to optimal control problems*. Longman Scientific and Technical, Harlow, 1991.

[13] John, B.T. *Practical methods for optimal control using nonlinear programming*. Society for Industrial and Applied Mathematics, Philadelphia, 2001.

[14] Kenneth, H., Frode, M. and Edvall, M.M. User's guide for tomlab/scos, *(http://tomopt.com/tomlab/products/socs/)*, 2006.

[15] Jennings, L.S., Fisher, M.E., Teo, K.L. and Goh, C.J. MISER3: Solving optimal control problems - an update, *Advance Engineering Software* (1991) 190–196.

[16] Prado, A.F.B.A. A survey on space trajectories in the model of three bodies. *Nonlinear Dynamics and Systems Theory* **6**(4) (2006) 389–400.

[17] Luenberger, D.G. The Gradient Projection Method Along Geodesics. *Management Science* **18**(11) (1972) 620–631.

[18] Teo, K.L., Jennings, L.S., Lee, H.W.J. and Rehbock, V. The control parameterization enhancing transform for constraint optimal control problems. *J. Austral. Math. Soc. Ser. B* 40 (1999) 314–335.